Centerline Boundary Dice Loss for Vascular Segmentation

Theoretical Analysis of clDice Variants. This section delves into the theoretical foundations and geometric sensitivities of cl-X-Dice metrics in vascular segmentation. We introduce three theorems to elucidate the behavior and computation of cl-X-Dice metrics:

Theorem 1. *For vertical translations along skeleton lines without deformation, cl-M-Dice coefficient is sensitive to translations of mask V within radius R, whereas clDice remains invariant.*

Proof. In 2D, cl-M-Dice is defined thus (extendable analogously to 3D):

$$\mathrm{Tprec}(S_{\mathrm{P}}, S_{\mathrm{L}}, V_{\mathrm{L}}) = \frac{|S_{\mathrm{P}} \cap D_{\mathrm{L}}|}{|R_{\mathrm{P}} \cap (U - S_{\mathrm{L}})| + |S_{\mathrm{P}} \cap R_{\mathrm{L}}|} \tag{1}$$

$$\mathrm{Tsens}(S_{\mathrm{L}}, S_{\mathrm{P}}, V_{\mathrm{P}}) = \frac{|S_{\mathrm{L}} \cap D_{\mathrm{P}}|}{|R_{\mathrm{L}} \cap (U - S_{\mathrm{P}})| + |S_{\mathrm{L}} \cap R_{\mathrm{P}}|} \tag{2}$$

Under vertical translations maintaining constant radius, $|S_{\mathrm{P}} \cap R_{\mathrm{L}}|$ equals $|S_{\mathrm{L}} \cap R_{\mathrm{P}}|$. This reduces cl-M-Dice's denominator to $|R_{\mathrm{P}}|$ (and analogously for R_{L}), making its sensitivity dependent solely on the numerator. Hence, cl-M-Dice reacts to spatial displacements of V within R. Conversely, clDice, assessing overlap between S and V, is not influenced by these variations.

Theorem 2. *cl-S-Dice, unlike clDice, is sensitive to radius variations at the skeleton under deformation without perpendicular translation. In cases of complete overlap, cl-S-Dice equals clDice with a value of 1.*

Proof. In 2D, cl-S-Dice is defined thus (extendable analogously to 3D):

$$\mathrm{Tprec}(S_{\mathrm{P}}, S_{\mathrm{L}}, V_{\mathrm{L}}) = \frac{|R_{\mathrm{P}} \cap V_{\mathrm{L}}|}{|R_{\mathrm{P}}|}, \quad \mathrm{Tsens}(S_{\mathrm{L}}, S_{\mathrm{P}}, V_{\mathrm{P}}) = \frac{|R_{\mathrm{L}} \cap V_{\mathrm{P}}|}{|R_{\mathrm{L}}|} \tag{3}$$

For clDice $\neq 1$ (partial overlap), changes in radius (R_{P}, R_{L}) affect both $|R_{\mathrm{P}} \cap V_{\mathrm{L}}|$ and $|R_{\mathrm{L}} \cap V_{\mathrm{P}}|$. Specifically, with $S = \{s_i, b_j^{\mathrm{s}} \mid i \in [1,n], j \in [1,m]\}$ and $R = \{r_i \cdot s_i, b_j^{\mathrm{s}} \mid, i \in [1,n], j \in [1,m]\}$, variances in r_i at any s_i modify cl-S-Dice. When clDice $= 1$ (complete overlap), $|R_{\mathrm{P}} \cap V_{\mathrm{L}}| = |R_{\mathrm{P}}|$ and $|R_{\mathrm{L}} \cap V_{\mathrm{P}}| = |R_{\mathrm{L}}|$, aligning cl-S-Dice with clDice, highlighting cl-S-Dice's sensitivity to radius changes in other scenarios.

Theorem 3. *cl-X-Dice enhances geometric sensitivity and compensates for diameter differences while preserving clDice's topological integrity.*

Proof. The cl-X-Dice metric, through the incorporation of variables $Q_{\mathrm{sl}}, Q_{\mathrm{sp}}, Q_{\mathrm{vl}}$, and Q_{vp}, offers an advanced sensitivity to geometric alterations, including size and shape variability, while upholding the topological preservation traits of clDice.

$$\mathrm{Tprec}(S_{\mathrm{P}}, S_{\mathrm{L}}, V_{\mathrm{L}}) = \frac{|Q_{\mathrm{sp}} \cap Q_{\mathrm{vl}}|}{|Q_{\mathrm{sp}} \cap Q_{\mathrm{spvp}} \cap (U - S_{\mathrm{L}})| + |Q_{\mathrm{sp}} \cap Q_{\mathrm{slvl}}|} \tag{4}$$

$$\mathrm{Tsens}(S_{\mathrm{L}}, S_{\mathrm{P}}, V_{\mathrm{P}}) = \frac{|Q_{\mathrm{sl}} \cap Q_{\mathrm{vp}}|}{|Q_{\mathrm{sl}} \cap Q_{\mathrm{slvl}} \cap (U - S_{\mathrm{P}})| + |Q_{\mathrm{sl}} \cap Q_{\mathrm{spvp}}|} \tag{5}$$

Eq. 4 and Eq. 5 represent a balanced approach, maintaining topological accuracy while adapting to geometric variances, thus achieving an equilibrium between topological integrity and geometric precision.

		CoW Anterior Variants			CoW Posterior Variants		
		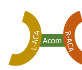			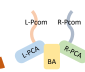	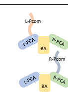	
		(n=11)	(n=2)	(n=5)	(n=4)	(n=6)	(n=8)
nnU-Net	CE+Dice	0%	0%	0%	0%	17%	50%
	CE+Dice+clDice	64%	50%	0%	75%	67%	75%
	CE+Dice+cbDice	64%	50%	40%	75%	83%	75%
SwinUNETR	CE+Dice	36%	0%	20%	100%	67%	50%
	CE+Dice+clDice	45%	50%	0%	75%	100%	63%
	CE+Dice+cbDice	45%	50%	20%	100%	100%	88%
NexToU	CE+Dice	55%	50%	40%	50%	50%	50%
	CE+Dice+clDice	73%	50%	40%	100%	67%	63%
	CE+Dice+cbDice	73%	50%	60%	100%	67%	75%

Table 1. CoW variant topology matching performance on the TopCoW 2023.

Category	Abbreviation	Full Name
Non-communicating arteries	BA	Basilar Artery
	R-PCA	Right Posterior Cerebral Artery
	L-PCA	Left Posterior Cerebral Artery
	R-ICA	Right Internal Carotid Artery
	R-MCA	Right Middle Cerebral Artery
	L-ICA	Left Internal Carotid Artery
	L-MCA	Left Middle Cerebral Artery
	R-ACA	Right Anterior Cerebral Artery
	L-ACA	Left Anterior Cerebral Artery
Communicating arteries	R-Pcom	Right Posterior Communicating Artery
	L-Pcom	Left Posterior Communicating Artery
	Acom	Anterior Communicating Artery
	3rd-A2	A2 segment of the Anterior Cerebral Artery

Table 2. Classification of the Cerebral Arteries in the Circle of Willis